

IONIZATION PHYSICS EVIDENCE FOR MAGNETIC FLARE ORIGIN OF THE X-RAYS IN AGN

SERGEI NAYAKSHIN¹

NASA/GSFC, LHEA, Code 661, Greenbelt, MD, 20771

Draft version November 2, 2018

ABSTRACT

We present full disk X-ray reflection spectra for two currently popular accretion flow geometries for AGN – the lamppost model frequently used to discuss the iron line reverberation in AGN, and the model where the X-rays are produced in magnetic flares above a cold accretion disk (AD). The lamppost spectra contain several spectroscopic features characteristic of highly ionized material that are not seen in the X-ray spectra of most AGN. The magnetic flare model, on the other hand, produces reflected spectra that are roughly a super-position of a power-law and a *neutral-like* reflection and iron K α line, and are thus more in line with typical AGN X-ray spectra. Furthermore, because of the difference in the ionization structure of the illuminated material in the two models, the line equivalent width increases with the X-ray luminosity, L_x , for the lamppost, and decreases with L_x for the flare model. In light of these theoretical insights, recent iron line reverberation studies of AGN, the X-ray Baldwin effect, and the general lack of X-ray reflection features in distant quasars all suggest that, for high accretion rates, the cold accretion disk is covered by a Thomson thick, *completely ionized* skin. Because the latter is only possible when the X-rays are concentrated to small emitting regions, we believe that this presents a strong evidence for the magnetic flare origin of X-rays in AGN.

Subject headings: accretion, accretion disks — radiative transfer — line: formation — X-rays: general

1. INTRODUCTION

Iron K α emission and the so-called reflection hump centered around ~ 30 keV are perhaps the only significant observational signatures of the presence of cold matter close to the event horizon around accreting black holes in Active Galactic Nuclei (AGN) and Galactic Black Hole Candidates (GBHC). This is why many theory papers investigated X-ray reflection spectra from AGN and GBHCs in great detail under the assumption that the matter is non-ionized or that the density of the illuminated layer is constant (e.g., Lightman & White 1988; George & Fabian 1991; Ross & Fabian 1993; Matt, Fabian & Ross 1993, 1996; Źycki et al. 1994, and additional references in NK). Basko, Sunyaev & Titarchuk (1974); Kallman & White (1989); Raymond (1993); Ko & Kallman (1994); Rózańska & Czerny (1996) relaxed the constant density assumption and all found that the thermal ionization instability (Krolik et al. 1981) plays a central role in establishing the equilibrium temperature and density profiles of the X-ray illuminated gas. Nayakshin, Kazanas & Kallman (2000; hereafter NKK) extended results of these authors by providing accurate radiation transfer for illuminating spectra appropriate for the inner part of ADs in AGN and GBHCs. The results of NKK show that a self-consistent gas density determination may provide valuable physical insights into the problem that allow one to put tight constraints on AD theories.

As an example, Nayakshin & Kallman (2000; NK hereafter) considered the X-ray illumination problem in the three different AD geometries: (1) the “lamppost” geometry, where the X-ray source is located above the black hole at some height h_x ; (2) full corona geometry (e.g., Liang & Price 1979) and (3) the two-phase patchy corona model (e.g., Galeev, Rosner & Vaiiana 1979; Haardt, Maraschi & Ghisellini 1994; and Svensson 1996). They pointed out that the reflected spectra and correlations between the X-ray continuum and the atomic features,

such as the Fe K α line and the associated edge are very different for these three geometries. Here we present the full disk spectra for the lamppost and the flare models and broadly compare our theoretical predictions to current observations of AGN. We find that a number of observational facts rules out the lamppost model geometry and, at the same time, supports the magnetic flare origin for the X-rays. (Note that we do not discuss here the Advection Dominated Accretion Flows (e.g., Ichimaru 1977; Rees et al. 1982; Narayan & Yi 1994) or modifications of this model due to winds (e.g., Blandford & Begelman 1999; Quataert & Gruzinov 2000) since these models are not expected to work for many luminous AGN that have broad iron lines – see the recent review by Fabian et al. [2000]).

2. GEOMETRY OF THE X-RAY SOURCE AND THE IONIZATION STATE OF THE DISK

Our main argument is based on two simple concepts. The first one has to do with geometrical differences between the lamppost and the flare models. In the former, the central X-ray source illuminates the disk “evenly” in the sense that the local illuminating flux at every radius is the same as the azimuthal average of that flux. In the case of flares, however, there may be many X-ray sources located anywhere above the inner AD and only several disk height scales above it (e.g., Galeev et al. 1979; Haardt, Maraschi & Ghisellini 1994; Nayakshin 1998). If the covering fraction of the disk by the flares is $f_c \ll 1$, then around the flare location (where most of the X-ray reflection takes place), the illuminating flux is roughly f_c^{-1} times larger than the average of that flux. Therefore, for the same X-ray luminosity, $L_x \sim L_d$, where L_d is the disk bolometric luminosity, the illuminating X-ray flux is $F_x \sim F_d$ and $F_x \gg F_d$, for the lamppost and flare models, respectively, where F_d is the intrinsic disk thermal flux (see also Fig. 1 and estimates in Nayakshin & Dove 2000).

The second point is that the Compton temperature – the max-

¹National Research Council Associate

imum gas temperature reached in the X-ray illuminated skin on the top of the disk – sensitively depends on the ratio F_x/F_d . Let T_x be the Compton temperature due to the illuminating X-radiation only, which for typical Seyfert Galaxies spectra work out to be around several to 10 keV. Then (e.g., Begelman, McKee & Shields 1983),

$$T_c = \frac{T_x J_x + T_{\text{eff}} J_{\text{BB}}}{J_x + J_{\text{BB}}} \approx \frac{T_x J_x}{J_x + J_{\text{BB}}}, \quad (1)$$

where we used $T_{\text{eff}} \ll T_x$, and where J_x and J_{BB} is the angle integrated intensity of the X-rays and the soft disk flux, respectively. Forgetting for the moment complications due to the angle averaging of radiation and its transfer through the skin, $J_x/J_{\text{BB}} \sim F_x/F_d$, and hence the geometry of the X-ray source directly influences T_c .

NK made these arguments more precise by solving the X-ray illumination problem at $R = 6R_s$ (R_s is the Schwarzschild radius) in the lamppost geometry with the following “reasonable” parameters: $h_x = 6R_s$, $\eta_x \equiv L_x/L_d = 1/5$, photon spectral index $\Gamma = 1.8$ and the exponential cutoff energy $E_c = 200$ keV. The gas temperature on the top of the skin turns out to be only $kT \lesssim 700$ eV. In contrast, in the magnetic flare case (NK assumed that $F_x/F_d \sim 100$), the gas temperature on the top of the skin to climb to about 4 keV (see Figs. 1 & 5 in NK). Not surprisingly, this large difference in the gas temperature leads to as profound a difference in the ionization structure of the gas. For the lamppost geometry, a large fraction of iron in the skin is in the form of Helium-like iron. For the flare case, on the other hand, the skin is dominated by the completely ionized iron. Figure 1a shows the ratio of the column depth of the He-like iron in the skin to that of the completely ionized iron for the lamppost and the flare models as a function of F_x/F_{x0} for runs w1-w9 and h1-h7 presented in NK, where F_{x0} is the illuminating X-ray flux of the test with the lowest value of L_x (w1 and h1, respectively). For the lamppost, He-like iron dominates by factor of few over completely ionized iron in the skin, whereas for the magnetic flare case, He-like ions are only few percent of the total iron line column depth in the skin.

The presence or absence of He-like iron in the skin makes it to play two opposite roles for the reflected spectra. Because He-like iron has much higher fluorescence yield than neutral-like iron below the skin, the warm skin yields a higher iron line emissivity than the one from a non-ionized matter. However, when the skin is completely ionized, it obstructs penetration of the incident X-rays to the cooler layers below where the Compton reflection hump and the fluorescent line are formed, and further wash out these features by Compton scattering when the line photons propagate through the skin to the observer (see NKK). Figure 1b shows the dependence of the iron K α equivalent width (EW) on the X-ray flux. Clearly, the dependence of the EW on F_x is opposite for the two models. In both cases, the Thomson depth of the skin increases with the X-ray luminosity (see Nayakshin 2000), but because the skin in lamppost model is He-like-dominated, this leads to an increase in the line’s EW, whereas for the completely ionized skin, it brings about a decrease in EW (the cool matter below the skin is less and less “visible”).

NK set several tests where they varied the ratio η_x to determine how high it should be to completely ionize the skin in the lamppost case. It turned out that this ratio needs to be as high as 10 or larger, because otherwise the gas temperature on the bottom of the skin falls far below the estimate given by equation 1 with $J_x/J_{\text{bb}} = F_x/F_d$ (see §6.3.1 and Figs. 13-15 in

NK). However, values of $\eta_x \gtrsim 1$ are in conflict with the fact that many AGN have UV fluxes exceeding their X-ray fluxes (e.g., NGC 3516, Edelson et al. 1999). Finally, NK showed that in the geometry of a full corona sandwiching the cold disk, the additional weight/pressure of the corona is so high that no ionized skin can form, and thus the reflected spectra should resemble those of a neutral reflector. The EW of the iron K α line is constant in this model (see Fig. 1b).

3. FULL DISK SPECTRA

In order to obtain full disk spectra, we calculate the local reflected spectra, I_k , with the code of NKK and NK for 6 different radii $r_k \equiv R/R_s = 3.5, 4.9, 7, 14, 35$ and 105. We assume that the reflected spectrum for $3 < r < r_1$ is given by that for $r = r_1$, and the one for $r > r_6$ is the one for $r = r_6$. Further, for radius $r_k < r < r_{k+1}$, we define the reflected spectrum to be

$$I(r) = \frac{\Delta r_{k+1} I_k + \Delta r_k I_{k+1}}{r_{k+1} - r_k}, \quad (2)$$

where $\Delta r_k = r - r_k$ and $\Delta r_{k+1} = r_{k+1} - r$. For simplicity of notations, we dropped the dependency of I_k on the cosine of the viewing angle, μ , and photon energy, E . In practice, we calculate the reflected spectrum for 10 different viewing angles θ_v that are measured from the normal to the disk, such that $\mu_v \equiv \cos \theta_v = 0.05, 0.15, \dots, 0.95$. We then interpolate in a linear fashion in μ_v (analogous to equation 2) to obtain the reflected spectrum for an intermediate value of μ_v .

The full spectra are obtained via integrating over the disk surface. To take into account the relativistic smearing in the Schwarzschild geometry of a non-rotating black hole, we include gravitational redshift in the photon energy and Doppler boosting due to Keplerian disk rotation, but we neglect the ray bending in the vicinity of the black hole. Since we only consider regions with $R > 3R_s = 6GM/c^2$, and since the maximum of the X-ray illuminating flux occurs at yet larger radii, we believe that this approximation is adequate for our study here. Both models are calculated for a 3×10^8 Solar masses black hole for dimensionless accretion rates: $\dot{m}_j = 2^{-(2j+1)}$, where $j = 0, 1, \dots, 4$ ($\dot{m} = 1$ corresponds to the Eddington luminosity). We assume $\eta_x = 1/3$, $\Gamma = 1.8$ and that the illuminating power-law extends to $E = 200$ keV where it is sharply cut.

It is perhaps fair to say that moderate to high luminosity lamppost spectra are rather unusual in that they display strong non-power-law features at soft X-ray energies, very strong He-like iron line at ~ 6.7 keV, and also a rather deep and high energy Fe absorption edge (blended with Fe Ly continuum, see NK). These are generally *not* observed in the spectra of real AGN or GBHCs. Note that the lower normalization of the reflected spectrum of the lamppost case compared with that for the magnetic flare case is due to two factors: (i) there is a hole underneath the lamppost so that a part of the flux never reflects; (ii) the X-ray continuum from magnetic flares is itself beamed along the disk surface and smeared so that the observer perpendicular to the disk observes less of the continuum flux than in the lamppost case for the same *intrinsic* L_x .

Figure 2b shows that below K α iron line feature, the magnetic flare spectra are practically pure power-laws, which is due to the fact that the skin is completely ionized. As shown by Done & Nayakshin (2000), spectra for the magnetic flare model can be fitted reasonably well by the standard single-zone reflection amid a lower normalization for the reflection hump, i.e.,

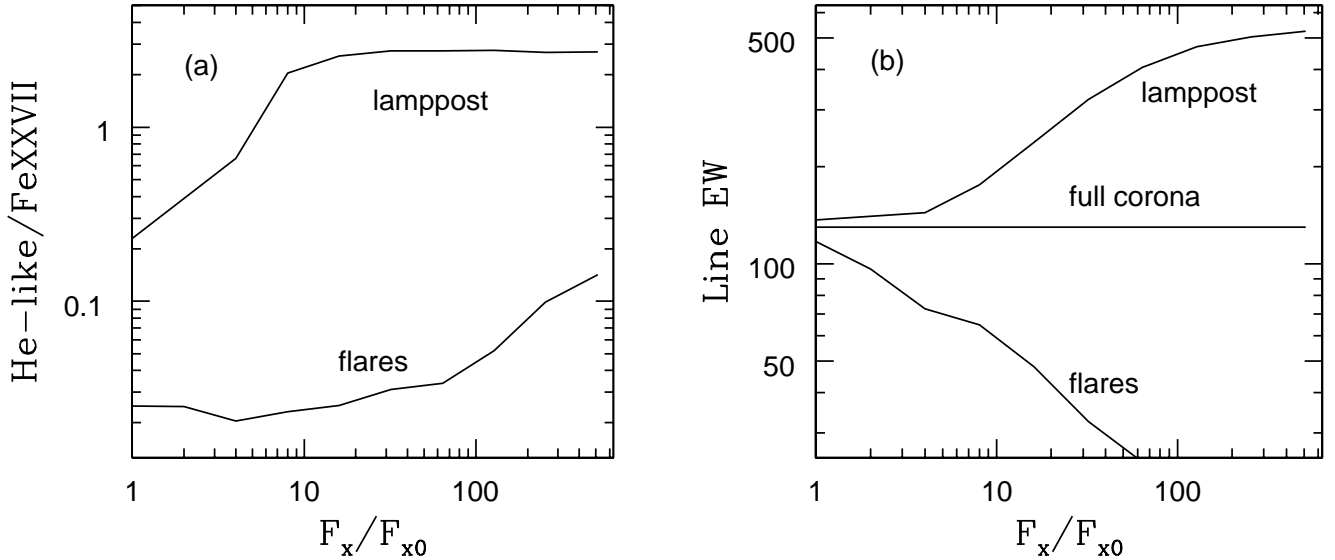


FIG. 1.— (a) – Ratio of He-like iron to the completely ionized iron in the skin for the lamppost and flare models as a function of the X-ray ionizing flux for the runs presented in NK. (b) – Behavior of the Equivalent Width (EW) of iron K α line for the three different models.

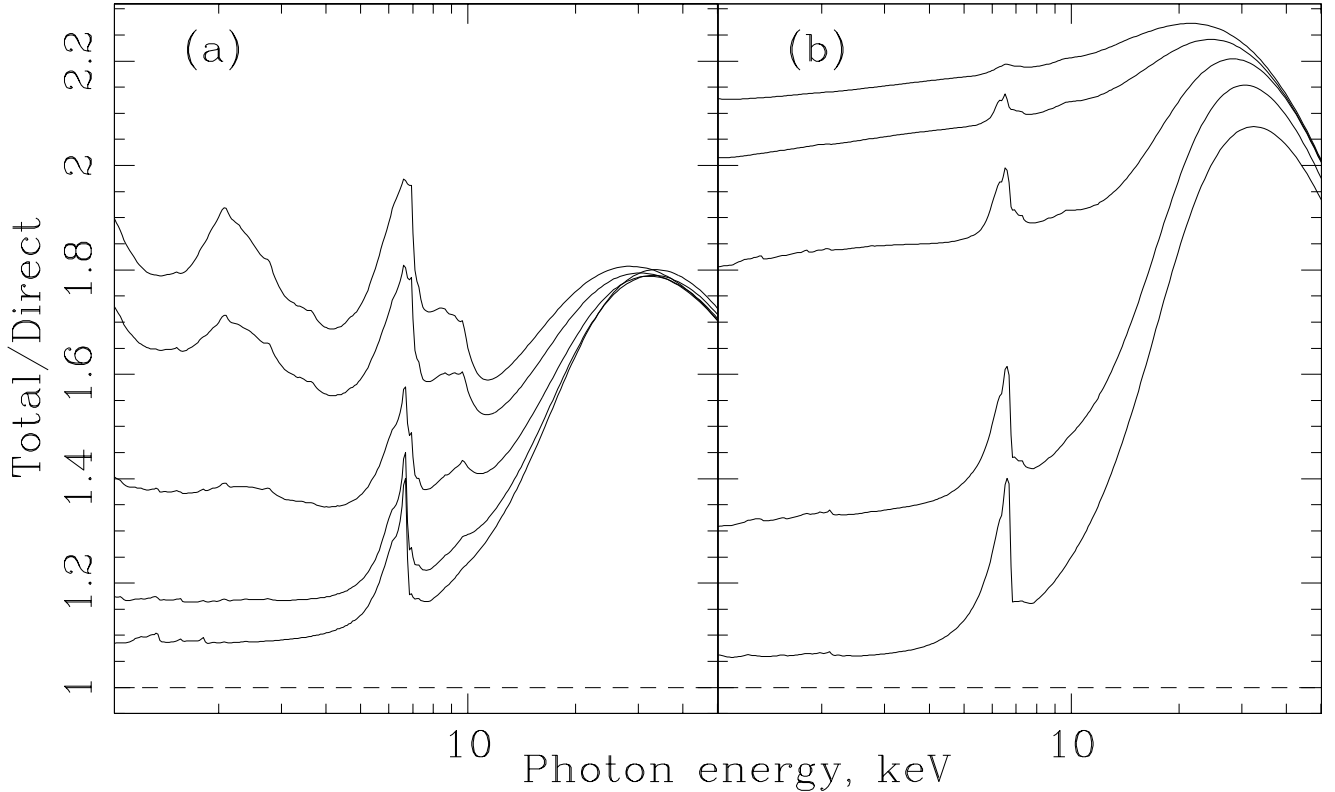


FIG. 2.— Ratio of the “observed” radiation intensity at an angle $\theta = 30^\circ$ to that from the X-ray source(s) only for (a) the lamppost model, and (b) the magnetic flare model. The dimensionless accretion rates are $\dot{m}_j = 2^{-(2j+1)}$, $j = 0, \dots, 4$, from top to bottom. Note that the lamppost spectra are never featureless because elements such as O, Mg, Si, S and Fe are not completely ionized. On the other hand, the reflected spectra for the magnetic flare model can be exact power-laws below $E \sim 20\text{ keV}$ because all these elements are completely ionized in the skin.

these spectra do appear to be similar to the typical AGN and even hard state GBHC spectra.

4. DISCUSSION

A search for the iron line reverberation in response to continuum variations was the goal of recent observations of MCG–6–30–15 (Lee et al. 2000; Reynolds 2000) and NGC 5548 (Chiang et al. 2000). These authors showed that whereas the continuum X-ray flux was strongly variable on short time scales, the iron $K\alpha$ line flux stayed roughly constant on these time scales and formally did not vary during the whole observation, which is far longer than the light crossing time of the innermost region. This seems to argue that the reflection takes place very far from the black hole – e.g., in the putative molecular torus. However, the line profile is *broad*, indicating that most of its flux does come from the region rather close to the black hole. According to Figure 1b, the lamppost geometry and the full corona case cannot explain the lack of iron line reverberation, because that requires the EW of the line to drop with increase in the X-ray flux approximately as $EW \propto F_x^{-1}$, whereas it increases with F_x for the lamppost model and stays constant for the full corona geometry. On the other hand, the magnetic flare model can potentially explain these interesting observations because the skin is completely ionized in this model and thus the EW of the line decreases with the X-ray flux.

Nandra et al. (1997) have shown that EW of the iron line monotonically decreases with the increasing L_x for a sample of AGN (the X-ray “Baldwin” effect). This study is corroborated by observations of Vignali et al. (1999) who found that the available data for luminous (high z) quasars indicate that the latter lack the reflection component and also have no or weak iron lines. This suggests that either there is no cold matter near the X-ray source, or it is hidden by a Thomson thick and completely ionized skin (as suggested by Nayakshin 2000). The former possibility would be somewhat unexpected because the currently popular AD theories either have the cold disk going all the way to the last stable orbit black hole (e.g., magnetic flares, lamppost) for all accretion rates, or suggest that the hot part of the accretion flow diminishes with increase in L and eventually disappears (e.g., Esin, McClintock & Narayan 1997; see also §6.1 in Fabian et al. 2000). In other words, in all these theories the luminous quasars are expected to have cold disk persisting down to the last stable orbit, and hence the absence

of the line and reflection have to be explained by the ionization physics effects (unless X-ray sources relativistically move away from the disk – see Beloborodov 1999 – the more so the higher L_x is). Out of the two models, the lamppost is clearly ruled out while the magnetic flare model seems quite viable.

Further, the full disk spectra (Fig. 2) show that the lamppost model predicts many strong features due to Oxygen, Mg, Si and other elements in soft X-rays, practically as prominent as those in the iron recombination band, and an enormous EW for the iron line, and a notably large iron absorption edge at ~ 9 keV. Such spectra are uncommon for real AGN, which again argues against the lamppost model. On the other hand, crudely speaking, the reflected spectra of the magnetic flare model is a combination of the mirror-like reflection from the completely ionized skin and the cold-like reflection hump and Fe $K\alpha$ line formed in the cold layers below the skin. These spectra do appear to be neutral (for $\Gamma \lesssim 2$, see NKK) and are reminiscent of spectra of real AGN and hard state GBHCs (see Done & Nayakshin 2000). In addition, while some Seyfert 1 AGN do have extremely broadened iron lines like MCG–6–30–15 (e.g. NGC 3516; Nandra et al. 1999), others do not have the extreme skewed lines expected from the very inner disk (e.g. IC4329a; Done, Madejski & Źycki 2000). As is clear from Figure 2b, the magnetic flare model can explain both of these facts if we suggest that broad iron line AGN are those with low $\dot{m} \lesssim 0.01$ or so, whereas narrow iron line AGN accrete at larger \dot{m} such that the skin in their inner disk completely destroys the broad line component. Note that the lamppost model again fails here, because its skin increases the line EW (see Fig. 2a).

Therefore, it emerges that the current observations indicate that the ionized skin is indeed present on the top of accretion disks in AGN and that it is *completely* ionized. The latter is only possible if the illuminating X-ray flux is much larger than the disk flux, which is most natural for accretion disks with magnetic flares occurring above the disk. The condition $F_x \gg F_d$ is in the fact the basic assumption of the two-patchy phase model (same as the magnetic flare model), because this requirement is central in producing the X-ray continuum spectra as hard as those observed and for a broad range of the parameter space (e.g., Haardt et al. 1994; Stern et al. 1995; Poutanen & Svensson 1996; Nayakshin & Dove 2000).

REFERENCES

Basko, M.M., Sunyaev, R.A., & Titarchuk, L.G. 1974, A&A, 31, 249
 Begelman, M.C., McKee, C.F., & Shields, G.A. 1983, ApJ, 271, 70
 Beloborodov, A.M. 1999, ApJ, 510, L123
 Blandford, R.D., & Begelman, M.C. 1999, MNRAS, 303, L1
 Done C., Madejski G.M., Źycki P.T., 2000, ApJ., in press.
 Done, C., & Nayakshin, S. 2000, submitted to ApJ.
 Edelson, R., et al. 1999, ApJ, 534, 180
 Esin A. A., McClintock J.E., Narayan R., 1997, ApJ., 489, 865
 Fabian, A.C., Iwasawa, K., Reynolds, C.S., & Young, A.J. 2000, PASP accepted (astro-ph/0004366)
 Galeev, A. A., Rosner, R., & Vaiana, G. S., 1979, ApJ, 229, 318
 George, I.M., & Fabian, A.C. 1991, MNRAS, 249, 352
 Haardt F., Maraschi, L., & Ghisellini, G. 1994, ApJ, 432, L95
 Ichimaru, S. 1977, ApJ, 214, 840
 Kallman, T.R., & White, N. E. 1989, ApJ, 341, 955
 Ko, Y-K., & Kallman, T.R. 1994, ApJ, 431, 273
 Krolik, J.H., McKee, C.F., & Tarter, C.B. 1981, ApJ, 249, 422
 Liang, E.P., & Price, R.H. 1977, ApJ, 218, 247
 Lightman, A.P., & White, T.R. 1988, ApJ, 335, 57
 Matt, G., Fabian, A.C., Ross, R.R. 1993, MNRAS, 262, 179
 Matt, G., Fabian, A.C., Ross, R.R. 1996, MNRAS, 278, 1111
 Nandra, K., George, I.M., Mushotzky, R.F., Turner, T.J., & Yaqoob, T. 1997, ApJ, 488, L91
 Nandra K., George I.M., Mushotzky R.F., Turner T.J., Yaqoob T., 1999, ApJ, 523, 17
 Nayakshin S. 1998, PhD thesis, University of Arizona
 Nayakshin S., & Dove, J.B. 2000, submitted to ApJ (astro-ph 9811059).
 Nayakshin, S. 2000, ApJ, 534, 718
 Nayakshin, S., Kazanas, D., & Kallman, T. 2000, to appear in ApJ volume 537.
 Nayakshin, S., & Kallman, T. 2000, submitted to ApJ (astro-ph/0005597)
 Poutanen, J., & Svensson, R. 1996, ApJ, 470, 249
 Quataert, E., & Gruzinov, A. 2000, to appear in ApJ (astro-ph/9908199)
 Raymond, J.C. 1993, ApJ, 412, 267
 Reynolds, C.S., & Begelman, M.C. 1997, ApJ, 488, 109
 Rees, M.J., Begelman, M.C., Blandford, R.D., & Phinney, E.S. 1982, Nature, 295, 17
 Reynolds, C.S., 2000, ApJ, 533, 811
 Ross, R.R., & Fabian, A.C. 1993, MNRAS, 261, 74
 Ross, R.R., Fabian, A.C., & Brandt, W.N. 1996, MNRAS, 278, 1082
 Ross, R.R., Fabian, A.C., & Young, A.J. 1999, MNRAS, 306, 461
 Rózańska , A., & Czerny, P.T. 1996, Acta Astron., 46, 233
 Stern, B., Poutanen, J., Svensson, R., Sikora, M., & Begelman, M. C. 1995, ApJ, 449, L13
 Svensson, R. 1996, A&A Supl., 120, 475
 Vignali, C., Comastri, A., Cappi, A., Palumbo, G.G.C., Matsuoka, M., & Kubo, H. 1999, ApJ, 516, 582
 Źycki , P.T., Krolik, J.H., Zdziarski, A.A., & Kallman, T.R. 1994, ApJ, 437, 597